



This open access document is published as a preprint in the Beilstein Archives with doi: 10.3762/bxiv.2020.92.v1 and is considered to be an early communication for feedback before peer review. Before citing this document, please check if a final, peer-reviewed version has been published in the Beilstein Journal of Organic Chemistry.

This document is not formatted, has not undergone copyediting or typesetting, and may contain errors, unsubstantiated scientific claims or preliminary data.

**Preprint Title** UV Resonance Raman Spectroscopy of the Supramolecular Ligand Guanidiniocarbonyl Indole (GCI) with 244 nm Laser Excitation

**Authors** Tim Holtum, Vikas Kumar, Daniel Sebena, Jens Voskuhl and Sebastian Schlücker

**Publication Date** 11 Aug 2020

**Article Type** Full Research Paper

**Supporting Information File 1** SI.pdf; 725.2 KB

**ORCID® IDs** Vikas Kumar - <https://orcid.org/0000-0002-7335-0824>; Daniel Sebena - <https://orcid.org/0000-0002-5828-5251>; Jens Voskuhl - <https://orcid.org/0000-0002-9612-2306>; Sebastian Schlücker - <https://orcid.org/0000-0003-4790-4616>

# UV Resonance Raman Spectroscopy of the Supramolecular Ligand Guanidiniocarbonyl Indole (GCI) with 244 nm Laser Excitation

Tim Holtum<sup>1</sup>, Vikas Kumar<sup>1</sup>, Daniel Sebens<sup>2</sup>, Jens Voskuhl<sup>2</sup>, Sebastian Schlücker<sup>1</sup> \*

Address:

<sup>1</sup>Physical Chemistry, Department of Chemistry and CENIDE, University of Duisburg-Essen, Universitätsstrasse 5, 45141 Essen, Germany

<sup>2</sup>Organic Chemistry, Department of Chemistry and CENIDE, University of Duisburg-Essen, Universitätsstrasse 7, 45141 Essen, Germany

Email: Sebastian Schlücker – [sebastian.schluecker@uni-due.de](mailto:sebastian.schluecker@uni-due.de)

\* Corresponding author

## Abstract

Ultraviolet resonance Raman (UVRR) spectroscopy is a powerful vibrational spectroscopic technique for label-free monitoring of molecular recognition of peptides or proteins with supramolecular ligands such as guanidiniocarbonyl pyrroles (GCPs). The use of UV laser excitation enables Raman binding studies of this class of supramolecular ligands at submillimolar concentrations in aqueous solution and provides a selective signal enhancement of their carboxylate binding site (CBS). A current limitation for the extension of this promising UVRR approach from peptides to proteins as binding partners for GCPs is the UV-excited autofluorescence from

aromatic amino acids observed for laser excitation wavelengths  $>260$  nm. These excitation wavelengths are in electronic resonance with the GCP for achieving both signal enhancement and selectivity for monitoring the CBS, but the resulting UVRR spectrum overlaps with UV-excited autofluorescence from aromatic binding partners. This necessitates the use of laser excitation  $<260$  nm for spectrally separating the UVRR spectrum of the supramolecular ligand from the UV-excited autofluorescence of the peptide or protein. Here, we demonstrate the use of UVRR spectroscopy with 244 nm laser excitation for the characterization of GCP as well as guanidiniocarbonyl indole (GCI), a next generation supramolecular ligand for recognition of carboxylates. For demonstrating the feasibility of UVRR binding studies without interference from the disturbing UV-excited autofluorescence, benzoic acid (BA) was chosen as an aromatic binding partner for GCI. We also present UVRR results from the binding of GCI to the ubiquitous RGD sequence (arginylglycylaspartic acid) as a biologically relevant peptide. In the case of RGD, the more pronounced differences between the UVRR spectra of free and complexed GCI (1:1 mixture) clearly indicate a stronger binding of GCI to RGD compared with BA. A tentative assignment of the experimentally observed changes upon molecular recognition is based on results from density functional theory (DFT) calculations.

## **Keywords**

Resonance Raman; UVRR; guanidiniocarbonyl pyrrole (GCP); Raman spectroscopy; guanidiniocarbonyl indole (GCI)

## Introduction

Supramolecular ligands are capable to selectively bind to peptides and proteins via reversible non-covalent interactions namely hydrogen bonds, van der Waals and/or hydrophobic interactions [1-5]. In this context, Schmuck and co-workers have introduced a class of synthetic receptors based on the guanidiniocarbonyl pyrrole (GCP) moiety (cf. Figure 1 top right) as a carboxylate binding site (CBS) [6-8]. The GCP takes part selectively and efficiently in the complexation of carboxylates based on the electrostatic interaction between the positively charged CBS and the negatively charged carboxylate in combination with hydrogen bonding, enabling molecular recognition even in the presence of polar solvents like water. This makes GCPs promising binding partners for acidic residues such as carboxylates at the C-terminus of peptides and proteins.

Intermolecular interactions upon recognition induce subtle changes in molecular properties such as electronic structure and bond strengths. Various spectroscopic techniques can be employed for monitoring these changes. For example, electronic absorption or fluorescence spectroscopy can probe the spectral differences due to the complexation of the supramolecular ligand with a peptide or protein. However, electronic spectroscopies probe the entire chromophore and are sensitive only to changes in the electronic structure of the molecule. In contrast, vibrational spectroscopic techniques such as infrared (IR) and Raman spectroscopy provide a much more detailed picture at the level of chemical bonds since they probe intrinsic vibrational modes of the molecule. Especially for non-covalent interactions such as hydrogen bonding, vibrational spectroscopy has been shown to be very sensitive [9-10]. In the context of supramolecular recognition, for example, IR spectroscopy has been applied to monitor the binding of tetrapeptides by GCP-based supramolecular

ligands containing also a tripeptide part for increasing selectivity [11]. However, IR spectroscopy does not provide selectivity for probing only the CBS. This is not critical as long as the binding partner is a small peptide, i.e., when the spectrum is not too crowded because of the small number of vibrational peaks. Additionally, IR spectroscopy suffers from the strong absorption by water. In contrast, this is not a problem in Raman spectroscopy because water is a weak Raman scatterer. Conventional Raman spectroscopy under non-resonant conditions is typically limited to millimolar concentrations due to small Raman scattering cross sections. Therefore, the biologically relevant submillimolar concentrations of GCP are not detectable by conventional (off-resonant) Raman spectroscopy. This limitation can be overcome by resonance Raman (RR) spectroscopy because it offers very high sensitivity owing to its enhanced Raman scattering from molecules that are in electronic resonance with the excitation laser frequency. In case of supramolecular recognition, this gives the additional advantage of selectivity where a molecular subunit can be selectively excited by properly choosing the laser wavelength in electronic resonance and the enhanced Raman spectrum involving only vibrational modes of the molecular subunit is selectively detectable. Since the GCP exhibits electronic resonances in the ultraviolet region with an absorption maximum at ca. 298 nm (see UV-Vis absorption spectrum of GCP in Figure 1 left), ultraviolet resonance Raman (UVRR) spectroscopy is employed for selectively enhancing the Raman signal from GCP subunit. UVRR spectroscopy gives signal enhancements by several orders of magnitude, enabling UVRR binding studies of GCP at submillimolar concentrations. In earlier studies, we have demonstrated the suitability of UVRR spectroscopy for monitoring supramolecular binding of monovalent GCP-based ligands with peptides [11-15] and a trivalent GCP-based ligand with the protein leucine zipper, a protein with a single aromatic unit [16], by using 275 and 266 nm laser excitation, respectively.

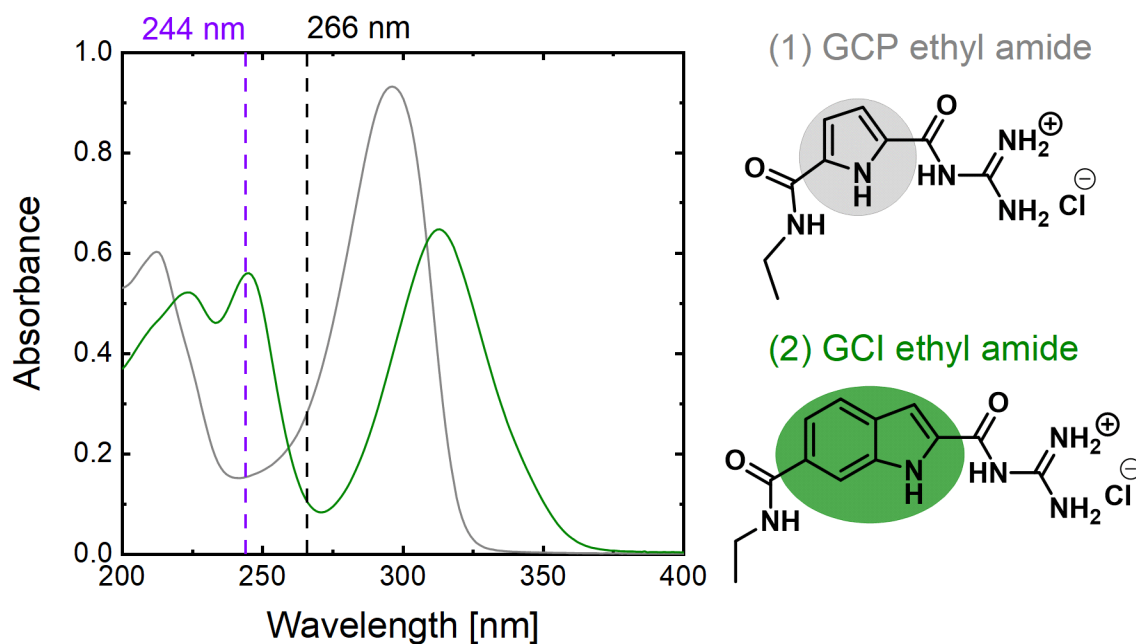


**Figure 1:** UV-Vis absorption spectra of GCP ethyl amide (in grey) and GCI ethyl amide (in green) at 200  $\mu\text{M}$  concentration in 6 mM BisTris buffer solution at pH 6. Excitation wavelengths used for UVRr experiments are indicated as dashed lines. The schematic molecular structures of protonated GCP ethyl amide and protonated GCI ethyl amide are also displayed. Substructures highlighted in grey and green are pyrrole and indole rings respectively.

The current challenge with UVRr spectroscopy for monitoring recognition of supramolecular ligands to proteins is the disturbing UV-excited autofluorescence from the aromatic amino acids. This autofluorescence typically occurs in the spectral range 260 – 440 nm and can significantly mask the spectrally overlapping UVRr signal. Due to this reason, UVRr binding studies so far were limited to the proteins with no or a minimal number of aromatic residues, for example, leucine zipper with one phenylalanine [16]. This problem can be circumvented either by temporally discriminating the Raman signal from the autofluorescence by using an optical switch such as a Kerr gate [17, 18], or by using short excitation wavelengths for spectrally

separating the UVRR signals from the UV-excited autofluorescence. The latter approach is achieved by sufficiently blue-shifting the UVRR spectrum away from the UV-excited autofluorescence [19, 20]. This is illustrated in Figure 2 for UVRR spectra of a 1 mM solution of toluene in acetonitrile acquired with 240, 258, 266 nm laser excitation. Spectra are plotted as a function of wavelength (rather than relative wavenumber/Raman shift) to illustrate the blue-shifting of UVRR spectral range of interest (0-3000  $\text{cm}^{-1}$ ) when moving towards lower excitation wavelengths. It can be seen that the spectral position of the UV-excited autofluorescence is independent of the choice of the excitation wavelength and that it overwhelms the detector even at a short integration time (0.9 s) for 258 and 266 nm excitations, masking the spectrally overlapped much weaker Raman signals. On the other hand, the 240 nm laser excitation spectrally isolates the UVRR spectral from the UV-excited autofluorescence. This allowed us to use a sufficiently high integration time (10 minutes) for obtaining good quality UVRR spectra at 244 nm excitation.

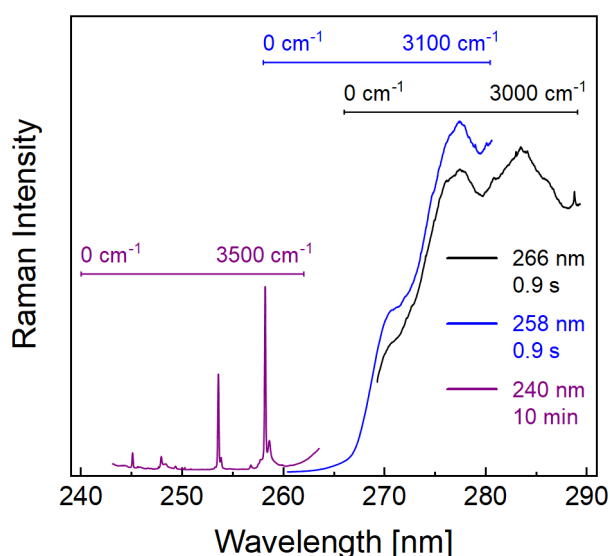


**Figure 2:** UVRR spectra of a 1 mM solution of toluene in acetonitrile acquired with 240, 258 and 266 nm laser excitation, respectively.

In this study, we evaluate the performance of UVRR spectroscopy with 244 nm laser excitation for the characterization of two guanidiniocarbonyl-based supramolecular ligands: guanidiniocarbonyl pyrrole (GCP) and guanidiniocarbonyl indole (GCI). The latter class of artificial carboxylate receptors is a potential next generation binder based on the GCI motif which maintains the good carboxylate binding properties of GCP. GCI comprises an indole ring instead of a pyrrole ring, which leads to different optical absorption properties in the UV-Visible range (see Figure 1). Based on the UV-Vis absorption spectrum, we expect a stronger resonance enhancement for GCI than GCP at 244 nm excitation due to its higher absorbance. Again, 244 nm excitation is necessary for spectrally separating the UVRR signal (below 260 nm) from the UV-excited autofluorescence starting from ca. 260 nm (cf. Fig. 2) [21]. We employ two different carboxylates for UVRR binding studies: benzoic acid (BA) as an aromatic model system and the ubiquitous RGD sequence (arginylglycylaspartic acid). BA was chosen in order to test experimentally whether UVRR at 244 nm laser excitation is free from UV-excited autofluorescence as expected from the initial results with toluene (Fig. 2). RGD was chosen as a biologically relevant tripeptide sequence highly abundant in proteins of the extracellular matrix.

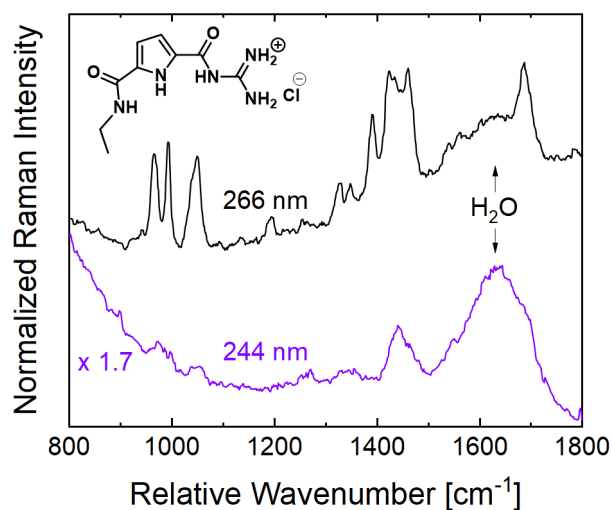
## Results and Discussion

Figure 1 (left) displays the absorption spectra of GCP ethyl amide and GCI ethyl amide at 200  $\mu$ M concentration in buffer. GCP ethyl amide shows a strong electronic absorption covering the entire spectral region below ca. 325 nm with two peaks at 298 and 215 nm. Both absorption bands can be attributed to  $\pi \rightarrow \pi^*$  transitions within the GCP chromophore. On the other hand, GCI ethyl amide exhibits a slightly red-shifted absorption band covering the entire region below 370 nm with two peaks at 320 and

244 nm which are also assigned to  $\pi \rightarrow \pi^*$  transitions of the GCI chromophore. The red-shift in the spectral positions of the GCI peaks with respect to those of the GCP peaks is due to the extended conjugation induced by the indole ring of GCI. We chose 266 nm and 244 nm as laser excitation wavelengths for UVRR spectroscopy. The 266 nm excitation was chosen because it has been employed in a recent UVRR binding study of a trivalent GCP-based ligand with the protein leucine zipper. The 244 nm excitation was chosen because this wavelength is sufficiently below the 260 nm minimum mark for avoiding spectral interference of UVRR with UV-excited autofluorescence and because it matches an intense electronic absorption peak of GCI. First, we performed UVRR spectroscopy on a 200  $\mu$ M GCP solution using 266 and 244 nm laser excitation (Figure 3). The UVRR spectrum with 266 nm excitation (black curve) shows characteristic strong Raman bands in the region 800-1800  $\text{cm}^{-1}$ . Peaks appearing within 1100 - 900  $\text{cm}^{-1}$  cover various pyrrole ring deformation modes while the peak at 1400  $\text{cm}^{-1}$  belongs to a symmetrical half ring vibration of pyrrole [12]. Based on results from DFT calculations [12], the peaks around 1470  $\text{cm}^{-1}$  are assigned to N-H bending and C-N stretch modes of both guanidinio and pyrrole. The peak at 1697  $\text{cm}^{-1}$  has a contribution from an Amide I-like vibration with C=O stretch contributions at the guanidiniocarbonyl part of the receptor.

In contrast, at 244 nm laser excitation only few, broad and featureless Raman peaks are observed (violet curve). This weaker resonance enhancement is due to the weaker electronic absorption of the GCP chromophore at 244 nm (see Fig. 1). The dominant and broad Raman band around 1640  $\text{cm}^{-1}$  is the deformation mode of water. This water band can also be seen in the 266 nm excited UVRR spectrum. Overall, due to the low signal enhancement in the UVRR spectrum obtained with 244 nm laser excitation, we did not perform any UVRR binding studies for GCP at the wavelength. Again, this

shorter excitation wavelength compared to 266 nm is necessary for circumventing the UV-autofluorescence occurring from aromatic binding partners.



**Figure 3:** UVRR spectra of a 200  $\mu\text{M}$  solution of GCP ethyl amide in 6 mM BisTris buffer solution at pH 6 acquired with 266 nm (black curve) and 244 nm (magenta curve) laser excitation.

We therefore performed a UVRR characterization of GCI at 266 nm and 244 nm laser excitation. From the strong electronic absorption of GCI (Fig. 1) a strong enhancement of the UVRR signal from GCI is expected for 244 nm excitation. Figure 4 shows the UVRR spectra obtained from a 200  $\mu\text{M}$  GCI solution using 266 and 244 nm laser excitation, respectively. In contrast to the spectra for GCP ethyl amide, both UVRR spectra of GCI ethyl amide show many sharp Raman bands. The intensities in the GCI UVRR spectrum with 244 nm laser excitation are twice as high compared to those in the UVRR spectrum recorded with 266 nm excitation. The strong signal for 244 nm excitation is explained by the higher absorbance of GCI at 244 nm compared to the absorbance at 266 nm. Both GCI UVRR spectra look very similar, exhibiting several distinct bands with the strongest peak around 1356  $\text{cm}^{-1}$ . Upon moving the laser excitation from 266 nm to 244 nm, two peaks around 996  $\text{cm}^{-1}$  and 1405  $\text{cm}^{-1}$  are

additionally enhanced and can be detected. Additionally, we observe a relative intensity increase for the band at  $1490\text{ cm}^{-1}$ .

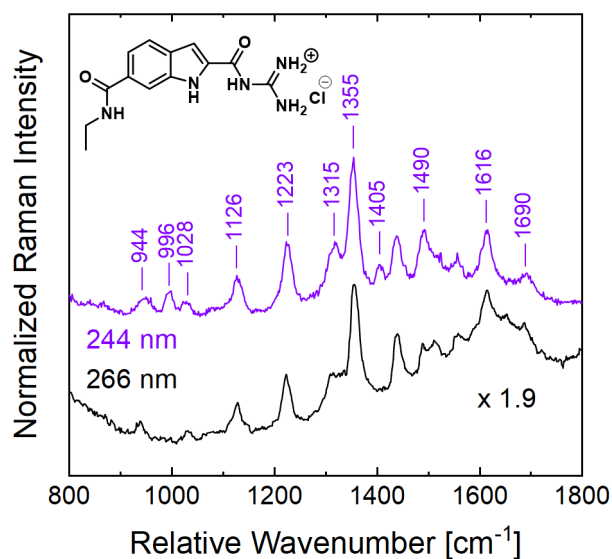


**Figure 4:** UVRR spectra of GCI ethyl amide at  $200\ \mu\text{M}$  concentration in  $6\ \text{mM}$  BisTris buffer solution at pH 6 acquired with  $266\ \text{nm}$  (black curve) and  $244\ \text{nm}$  (magenta curve) laser excitations.

For a peak assignment of the experimental UVRR spectrum of GCI, we employed results from density functional theory (DFT) calculations. The assignment of peaks detectable in the experimental UVRR spectrum is mainly based on its experimental wavenumber position (peak position). Only normal modes with non-vanishing Raman activities were considered. One cannot expect an agreement between experimental and theoretical intensities since the DFT calculations do not include the electronic resonance enhancement, which was exploited in the UVRR experiments.

Figure 5 presents the theoretical Raman spectrum of GCI ethyl amide molecule in the region  $800\text{-}1800\ \text{cm}^{-1}$  calculated at the B3LYP/6-311++G(d,p) level of theory. A complete list of the calculated vibrational modes along with their wavenumber positions and corresponding Raman activities is available in the Supporting Information (SI). Overall, there is a good agreement between the positions of the eleven peaks labeled

in the UVRR spectra in Figure 4 and the calculated wavenumbers after multiplication with a global scaling factor:

944  $\text{cm}^{-1}$  (theo. 930  $\text{cm}^{-1}$ ), 996  $\text{cm}^{-1}$  (theo. 1011  $\text{cm}^{-1}$ ), 1028  $\text{cm}^{-1}$  (theo. 1033  $\text{cm}^{-1}$ ), 1126  $\text{cm}^{-1}$  (theo. 1115  $\text{cm}^{-1}$ ), 1223  $\text{cm}^{-1}$  (theo. 1227  $\text{cm}^{-1}$ ), 1315  $\text{cm}^{-1}$  (theo. 1335  $\text{cm}^{-1}$ ), 1355  $\text{cm}^{-1}$  (theo. 1356  $\text{cm}^{-1}$ ), 1405  $\text{cm}^{-1}$  (theo. 1405  $\text{cm}^{-1}$ ), 1490  $\text{cm}^{-1}$  (theo. 1501  $\text{cm}^{-1}$ ), 1615  $\text{cm}^{-1}$  (theo. 1616  $\text{cm}^{-1}$ ) and 1690  $\text{cm}^{-1}$  (theo. 1695  $\text{cm}^{-1}$ ).

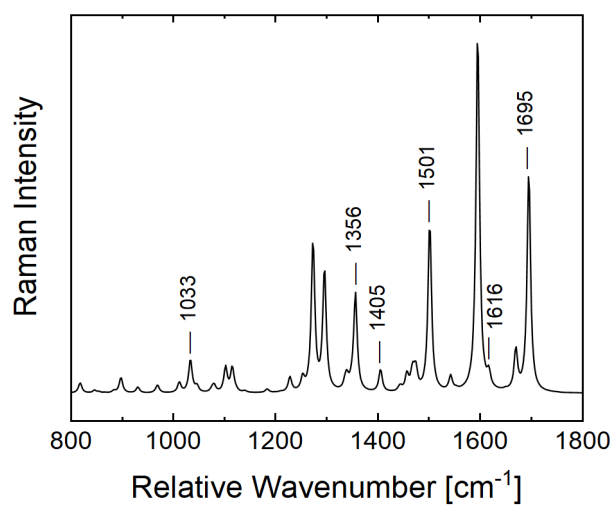


**Figure 5:** DFT calculated Raman spectrum of GCI ethyl amide plotted in the region 800-1800  $\text{cm}^{-1}$ . The positions of selected Raman peaks are indicated.

However, as expected, the relative intensities of the modes in the experimental UVRR spectra cannot be properly predicted by theory which calculated nonresonant Raman intensities. Calculating UVRR spectra for a complex molecule such as GCI is very challenging and beyond the scope of this paper.

Figure 6 shows DFT-calculated eigenvectors of six selected GCI modes at 1033  $\text{cm}^{-1}$ , 1356  $\text{cm}^{-1}$ , 1405  $\text{cm}^{-1}$ , 1501  $\text{cm}^{-1}$ , 1616  $\text{cm}^{-1}$  and 1695  $\text{cm}^{-1}$  which show a significant involvement of the guanidinio group. The 1033  $\text{cm}^{-1}$  peak has a contribution from a rocking motion of the guanidinio group extending to the pyrrole part of the indole ring (symmetric C-N stretching and asymmetric N-H bending), while the peak at 1356  $\text{cm}^{-1}$

belongs to vibrations mainly located at guanidinio group C-N stretch and N-H bending (amide III like). The  $1405\text{ cm}^{-1}$  peak can be attributed mainly to a stretching mode of the indole ring (similar to fundamental mode  $\nu_{12}$  of indole in ref. [22]), and additionally to N-H bending at the guanidinio group. The peak at  $1501\text{ cm}^{-1}$  has a major contribution from the dominant in-plane ring stretching mode of indole ( $\nu_{10}$  in ref. [22]) and N-H bendings from all N-H groups (peptide, indole, guanidinio) as well as a minor contribution from C-N stretch. The mode at  $1616\text{ cm}^{-1}$  consists of C-N stretching and N-H bending located at the guanidinio group, while the one at  $1694\text{ cm}^{-1}$  belongs to the amide I like vibration involving C=O stretch at the guanidiniocarbonyl part of the receptor. Vibrational assignment of these modes is important for binding study of GCI receptors because we hypothesize that they are all involved in complexation with carboxylates.

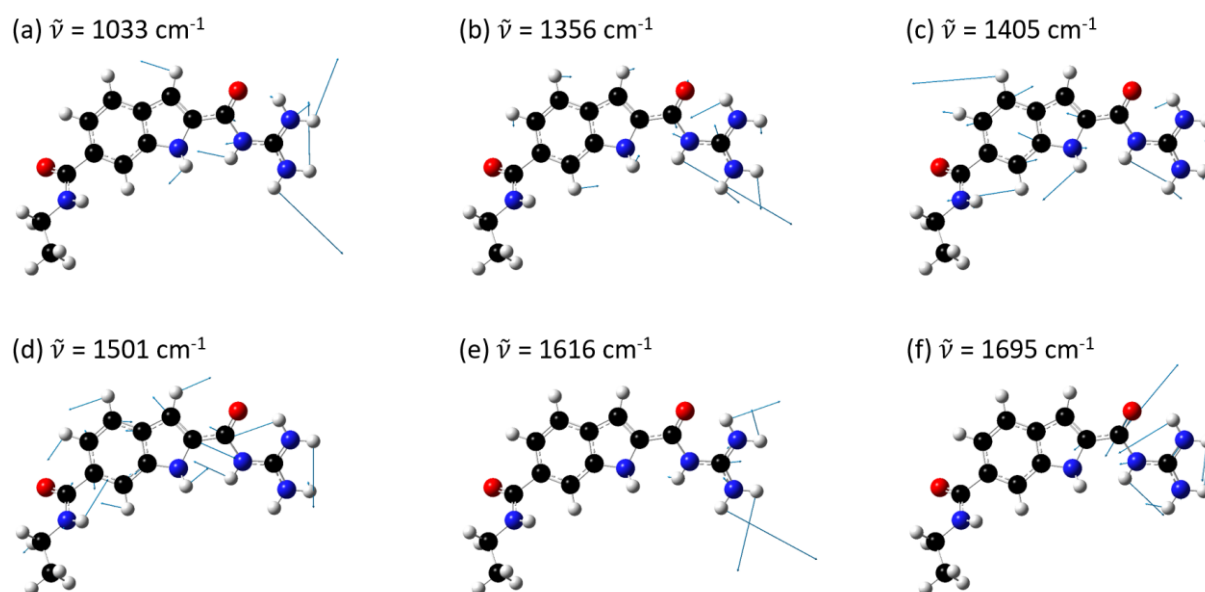


**Figure 6:** DFT computed eigenvectors of GCI ethyl amide of selected normal modes (cf. Figure 5) at (a)  $1033\text{ cm}^{-1}$ , (b)  $1356\text{ cm}^{-1}$ , (c)  $1404\text{ cm}^{-1}$ , (d)  $1501\text{ cm}^{-1}$ , (e)  $1616\text{ cm}^{-1}$  and (f)  $1694\text{ cm}^{-1}$ .

Finally, we employed UVRR spectroscopy at 244 nm excitation to observe binding events of GCI-based receptors using two different carboxylates as binding partners. We choose an aromatic binding partner, benzoic acid, for which the UV-excited autofluorescence might disturb the Raman signal at higher excitation wavelengths. For the second binding experiment we choose a biologically relevant peptide, RGD.

In the first experiment, the UVRR spectrum of a 1:1 mixture of benzoic acid and GCI ethyl amide (both 200  $\mu\text{M}$ ) was acquired with 244 nm laser excitation (shown as blue curve in Figure 7). This spectrum is compared to the UVRR spectra of the corresponding binding partners GCI ethyl amide (200  $\mu\text{M}$ , black curve in Figure 7 bottom) and of BA (200  $\mu\text{M}$ , Figure 7 top) both acquired maintaining the same experimental conditions. All three spectra were normalized to the Raman peak of water (OH stretching) around 3400  $\text{cm}^{-1}$ . The UVRR spectra of GCI+BA mixture and GCI show similar features with slight variations in intensity levels. To highlight the changes between the two spectra, the difference spectrum is plotted in Figure 7 middle. Prominent changes can be observed at 1596  $\text{cm}^{-1}$ , 1490  $\text{cm}^{-1}$  and 1356  $\text{cm}^{-1}$ . The band at 1596  $\text{cm}^{-1}$  can be assigned to BA. However, the band at 1356  $\text{cm}^{-1}$  which belongs to vibrations of guanidinio group C-N stretch and N-H bending, and the band at 1501  $\text{cm}^{-1}$  which has the major contribution from the dominant ring stretching mode of indole, are expected to take part in carboxylate binding. The observation of intensity variations for these bands indicates the carboxylate binding of GCI and BA. However, such subtle changes suggest that BA is a weak binding partner for GCI for molecular recognition.

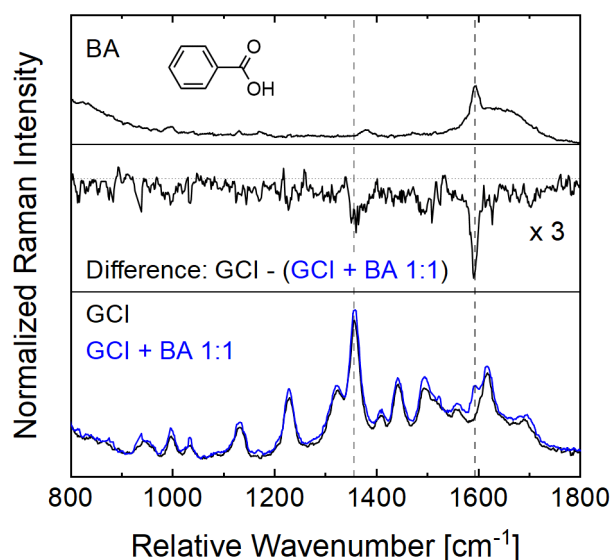


**Figure 7:** UVRR spectra obtained with 244 nm laser excitation: GCI and 1:1 mixture of 'GCI and BA' (bottom), difference spectrum (middle), and BA (top). The dashed lines mark the most prominent changes in the difference spectrum.

In a second binding experiment, we used the biologically relevant tripeptide RGD as a binding partner. The UVRR spectrum of a 1:1 mixture of RGD and GCI ethyl amide (both 200  $\mu\text{M}$ ) was acquired with 244 nm laser excitation (figure 8 blue curve). For comparison, the UVRR reference spectra of the two isolated components, i.e., 200  $\mu\text{M}$  GCI (figure 8 bottom black curve) and 200  $\mu\text{M}$  RGD (figure 8 top), were also recorded maintaining the same experimental conditions. All three spectra were then normalized to the Raman peak of water (OH stretching) at ca. 3400  $\text{cm}^{-1}$ . A comparison of the UVRR spectrum of the 1:1 mixture of GCI and RGD with the GCI reference spectrum shows strong intensity variations across a wide spectral range. Overall, these intensity changes are much more pronounced compared to the binding experiment with BA, where intensity variations just for few particular bands were observed (Fig. 7). The difference spectrum (Figure 8 middle) shows strong peaks at 1033  $\text{cm}^{-1}$ , 1120  $\text{cm}^{-1}$ , 1225  $\text{cm}^{-1}$ , 1310  $\text{cm}^{-1}$ , 1356  $\text{cm}^{-1}$ , 1405  $\text{cm}^{-1}$ , 1450  $\text{cm}^{-1}$ , 1501  $\text{cm}^{-1}$ , 1616  $\text{cm}^{-1}$  and 1695  $\text{cm}^{-1}$ . Thus, the corresponding normal modes of these peaks are

involved in complexation of the GCI. For six of these peaks the calculated eigenvectors in Fig. 6 clearly show an involvement of vibrations with contributions located at the indole ring and/or the guanidino moiety. Overall, the more pronounced changes in terms of larger intensities in the difference spectrum also suggest that RGD is a stronger binding partner to GCI as compared to BA. This is expected due to the fact that RGD has two carboxylic groups per molecule as compared to only one in BA (cf. molecular structures of BA and RGD in Fig. 7 and 8 respectively).

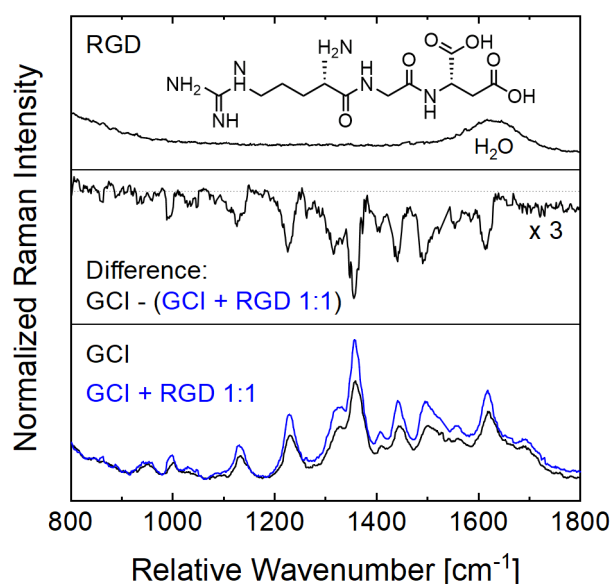


**Figure 8:** UVRR spectra obtained with 244 nm laser excitation: GCI and 1:1 mixture of 'GCI and RGD' (bottom), difference spectrum (middle), and RGD (top).

## Conclusion

Applying UVRR for label-free monitoring of molecular recognition of proteins by supramolecular ligands requires that the UV-induced autofluorescence is circumnavigated. This can be realized either in the time domain by using a UV Kerr-gate for temporally separating the Raman scattering from the time-delayed fluorescence or in the frequency domain by using shorter excitation wavelengths for blue-shifting the UVRR signal away from the UV-excited autofluorescence. In this

study, we have demonstrated the performance of UVRR spectroscopy with 244 nm and 266 nm laser excitation for two supramolecular ligands: GCP and GCI as a next generation binder. We have shown that for GCI the second option in the frequency domain works since the resonance enhancement is sufficient. However, for GCP this does not work due to the insufficient resonance enhancement. We also observed GCI binding events with two distinct binding partners: BA and RGD. RGD is found to be a stronger binding partner for GCI. We employed results from DFT for an assignment of the peaks in the experimental UVRR spectrum of GCI. For future UVRR binding studies with proteins using the GCP motif, the development of a Kerr-gate operating in the UV below 300 nm is required.

## Experimental

For 244 nm laser excitation a pulsed laser source (Light Conversion; Orpheus-PS, SHBC, LYRA) providing pulses at 10 kHz repetition rate with wavelength continuously tunable in 210 – 350 nm UV region was employed. For 266 nm laser excitation a continuous wave (CW) laser source (CryLaS GmbH, FQCW 266) was used. The UVRR spectrometer comprises a 50 cm focal length grating monochromator (Action Research Corp., SpectraPro-500i, 2400 grooves/mm grating) equipped with a cryogenically-cooled CCD sensor (Princeton Instruments, PyLoN:2K).

To avoid the possible interference by sample container material and to eliminate sample degradation by excess exposure to UV light, the liquid sample was circulated in a home-built free-flow system similar to one employed for deep UVRR studies [23]. This closed-loop system is driven by a peristaltic pump. A half air-filled syringe acts as an upper reservoir to flatten pressure oscillations from the peristaltic pump. An injection needle with 0.8 mm outer diameter is attached to the syringe as the output

nozzle to form a laminar liquid column in air at the laser focus. The laser radiation was focused by two cylindrical lenses to create a line focus along the sample liquid column and a 90° scattering geometry was used for collecting the Raman scattered light.

UV-Vis absorption spectra were acquired with a UV/VIS spectrometer (Perkin-Elmer Lambda 650) where liquid samples were kept in 2 mm fused silica cuvettes (Hellma).

DFT calculations were performed with the GAUSSIAN 2016 program package [24] with the B3LYP functional and the 6-311++G(d,p) basis set. The molecule was calculated in gas phase in its protonated form with one positive net charge. The resulting wavenumber values were scaled by a factor of 0.964 [25]. A FWHM of 4 cm<sup>-1</sup> and a Lorentzian line shape were used for simulating the theoretical spectrum in Fig. 5.

The GCP building block was synthesized according to a known literature procedure [26], followed by further functionalization with ethyl amine at the carboxylic acid in two steps to obtain GCP ethyl amide. The novel building block for GCI was synthesized in a 4-step synthesis adapted from a previous work [27] and then functionalized accordingly, yielding GCI ethyl amide (for detailed synthesis routes see Scheme S1 and Scheme S2 in the SI). The functionalization of the binding motifs GCP and GCI were performed since in the presence of the free guanidinium moiety the free carboxylic acid leads to strong dimerization based on zwitterion formation at neutral pH, as described for GCP ( $K_{dim} > 10^2$  in water) [28] as well as for a GCI derivative [29], which would interfere with anion binding.

Solid benzoic acid and RGD were purchased from Fluka Analytical and Sigma-Aldrich, respectively. Both chemicals were used without further purification. All liquid samples were prepared in 200 μM concentration in 6 mM BisTris buffer at pH 6.

## Supporting Information

DFT calculated normal modes with corresponding wavenumbers and Raman activities of GCI ethyl amide and detailed synthesis routes for GCP and GCI ethyl amide.

Supporting Information File 1:

File Name: SI.pdf

File Format: PDF

Title: DFT calculation results and detailed synthesis routes

## Acknowledgements

J.V. would like to thank Sarah Lampe for her contribution in development of the synthesis route for the GCI ethyl amide.

## Funding

This work is funded by the German Research Foundation (Collaborative Research Centre CRC 1093 “Supramolecular Chemistry on Proteins”, projects A1, A9 and A10).

## Conflicts of Interest

The authors declare no competing financial interest.

## References

1. Lehn, J-M *Science* **1985**, 227 (4689) 849-856.
2. Bier, D.; Mittal, S.; Bravo-Rodriguez, K.; Sowislok, A.; Guillory, X.; Briels, J.; Heid, C.; Bartel, M.; Wettig, B.; Brunsveld, L.; Sanchez-Garcia, E.; Schrader, T.; Ottmann, C. *Journal of the American Chemical Society* **2017**, 139 (45), 16256-16263.
3. Gale, P. A. *Chemical Communications* **2011**, 47 (1), 82-86.
4. Schmidtchen, F. P. *Chemical Society Reviews* **2010**, 39 (10), 3916-3935.

5. Wenzel, M.; Hiscock, J. R.; Gale, P. A. *Chemical Society Reviews* **2012**, 41 (1), 480-520.
6. Qian-Qian, J.; Wilhelm, S.; Martin, E.; Schmuck, C. *Chemical Science* **2015**, 6, 1792-1800.
7. Schmuck, C. *Chemistry – A European Journal* **2000**, 6 (4), 709-718.
8. Vallet, C.; Aschmann, D.; Beuck, C.; Killa, M.; Meiners, A.; Mertel, M.; Ehlers, M.; Bayer, P.; Schmuck, C.; Giese, M.; Knauer, S. K. *Angewandte Chemie International Edition* **2020**, 59 (14), 5567-5571.
9. Schlücker, S.; Singh, R. K.; Asthana, B. P.; Popp, J.; Kiefer, W. *Journal of Physical Chemistry A* **2001**, 105 (43), 9983-9989.
10. Schlücker, S.; Koster, J.; Singh, R. K.; Asthana, B. P. *Journal of Physical Chemistry A* **2007**, 111 (24), 5185-5191.
11. Niebling, S.; Kuchelmeister, H. Y.; Schmuck, C.; Schlücker, S. *Chemical Science* **2012**, 3, 3371-3377.
12. Küstner, B.; Schmuck, C.; Wich, P.; Jehn, C.; Srivastava, S. K.; Schlücker, S. *Physical Chemistry Chemical Physics* **2007**, 9, 4598-4603.
13. Srivastava, S. K.; Niebling, S.; Küstner, B.; Wich, P.; Schmuck, C.; Schlücker, S. *Physical Chemistry Chemical Physics* **2008**, 10, 6770-6775.
14. Niebling, S.; Srivastava, S. K.; Herrmann, C.; Wich, P.; Schmuck, C. Schlücker, S. *Chemical Communications* **2010**, 46, 2133-2135.
15. Niebling, S.; Kuchelmeister, H. Y.; Schmuck, C.; Schlücker, S. *Chemical Communications* **2011**, 47, 568-570.
16. Zakeri, B.; Niebling, S.; Martínéz, A. G.; Sokkar, P.; Sanchez-Garcia, E.; Schmuck, C.; Schlücker, S. *Physical Chemistry Chemical Physics* **2018**, 20, 1817-1820.
17. Matousek, P.; Towrie, M.; Parker, A. W., *Journal of Raman Spectroscopy* **2002**, 33, 238-242.
18. Blake, J. C.; Nieto-Pescador, J.; Li, Z.; Gundlach, L. *Optics Letters* **2016**, 41 (11), 2462-2465.
19. Bowman, W. D.; Spiro, T. G. *Journal of Raman Spectroscopy*, **1980**, 9 (6), 369-371.
20. Sands, H., Hayward, I., Kirkbride, T., Bennett, R., Lacey, R., and Batchelder, D. *Journal of Forensic Sciences* **1998**, 43 (3), 509-513.
21. Teale, F. W. J.; Weber, G. *The Biochemical Journal* **1957**, 65 (3), 476-482.
22. Majoube, M.; Vergoten, G. *Journal of Raman Spectroscopy* **1992**, 23, 431-444.
23. Bröermann, A.; Schlücker, S. *Zeitschrift für Physikalische Chemie* **2011**, 225, 691-701.
24. Frisch, M. J.; Trucks, G. W.; Schlegel, H. B.; Scuseria, G. E.; Robb, M. A.; Cheeseman, J. R.; Scalmani, G.; Barone, V. Petersson, G. A.; Nakatsuji, H.; et al., *Gaussian 16*, Rev. B01, Wallingford, CT, **2016**.
25. Kashinski, D. O.; Chase, G. M.; Nelson, R. G.; Di Nallo, O. E.; Scales, A. N., VanderLey, D. L.; Byrd, E. F. C. *The Journal of Physical Chemistry A* **2017**, 121, 2265-2273.
26. Schmuck, C.; Bickert, V.; Merschky, M.; Geiger, L.; Rupprecht, D.; Dudaczek, J.; Wich, P.; Rehm, T.; Machon, U. *European Journal of Organic Chemistry* **2008**, 324-329.
27. Rether C.; Schmuck, C. *European Journal of Organic Chemistry* **2011**, 1459-1466.
28. Schmuck, C.; Wienand, W. *Journal of the American Chemical Society* **2003**, 125, 452-459.
29. Rether, C.; Sicking, W.; Boese, R.; Schmuck, C. *Beilstein Journal of Organic Chemistry* **2010**, 6, 3.